

Water Permeability of Asymmetric Planar Lipid Bilayers: Leaflets of Different Composition Offer Independent and Additive Resistances to Permeation

ANDREY V. KRYLOV,¹ PETER POHL,¹ MARK L. ZEIDEL,² and WARREN G. HILL²

¹Nachwuchsgruppe Biophysik, Forschungsinstitut fuer Molekulare Pharmakologie, 13125 Berlin, Germany

²Renal-Electrolyte Division, Department of Medicine, University of Pittsburgh School of Medicine, Pittsburgh, PA 15261

ABSTRACT To understand how plasma membranes may limit water flux, we have modeled the apical membrane of MDCK type 1 cells. Previous experiments demonstrated that liposomes designed to mimic the inner and outer leaflet of this membrane exhibited 18-fold lower water permeation for outer leaflet lipids than inner leaflet lipids (Hill, W.G., and M.L. Zeidel. 2000. *J. Biol. Chem.* 275:30176–30185), confirming that the outer leaflet is the primary barrier to permeation. If leaflets in a bilayer resist permeation independently, the following equation estimates single leaflet permeabilities: $1/P_{AB} = 1/P_A + 1/P_B$ (Eq. 1), where P_{AB} is the permeability of a bilayer composed of leaflets A and B, P_A is the permeability of leaflet A, and P_B is the permeability of leaflet B. Using Eq. 1 for the MDCK leaflet-specific liposomes gives an estimated value for the osmotic water permeability (P_f) of 4.6×10^{-4} cm/s (at 25°C) that correlated well with experimentally measured values in intact cells. We have now constructed both symmetric and asymmetric planar lipid bilayers that model the MDCK apical membrane. Water permeability across these bilayers was monitored in the immediate membrane vicinity using a Na^+ -sensitive scanning microelectrode and an osmotic gradient induced by addition of urea. The near-membrane concentration distribution of solute was used to calculate the velocity of water flow (Pohl, P., S.M. Saparov, and Y.N. Antonenko. 1997. *Biophys. J.* 72:1711–1718). At 36°C, P_f was $3.44 \pm 0.35 \times 10^{-3}$ cm/s for symmetrical inner leaflet membranes and $3.40 \pm 0.34 \times 10^{-4}$ cm/s for symmetrical exofacial membranes. From Eq. 1, the estimated permeability of an asymmetric membrane is 6.2×10^{-4} cm/s. Water permeability measured for the asymmetric planar bilayer was $6.7 \pm 0.7 \times 10^{-4}$ cm/s, which is within 10% of the calculated value. Direct experimental measurement of P_f for an asymmetric planar membrane confirms that leaflets in a bilayer offer independent and additive resistances to water permeation and validates the use of Eq. 1.

KEY WORDS: MDCK cells • apical membrane • fluidity • cell membrane permeability • barrier function

INTRODUCTION

The process of water permeation across lipid membranes has significant implications for cellular physiology and homeostasis (Finkelstein, 1987). Multicellular organisms in particular are confronted with the necessity of compartmentalizing fluid volumes with differing compositions and osmolalities, e.g., in the gastrointestinal tract and the kidney. Since water will partition into phospholipid bilayers and diffuse across in response to osmotic pressure, organisms that need to maintain internal gradients have been forced to evolve specialized membranes that will impede the equilibration of water between compartments. These are often termed barrier membranes and are characterized by low water and solute permeability.

Although the precise structural features of barrier membranes responsible for reducing water and solute

fluxes are not entirely clear, some common features have emerged in recent studies. Water permeability has been shown to correlate strongly with membrane fluidity (Lande et al., 1995), therefore, it is necessary for the cell to construct a lumen-facing membrane that has high microviscosity. This can be achieved by: the inclusion of cholesterol, which tightens the packing of fatty acid aliphatic chains near the phospholipid head groups (Smaby et al., 1994); increasing the degree of acyl chain saturation; and using sphingolipids, which, by virtue of the unconventional amide linkage, are able to form hydrogen bonds with each other and with cholesterol (Smaby et al., 1996; Hill and Zeidel, 2000). In addition, cells are able to maintain membrane lipid asymmetry by incorporating different lipids into the outer and inner leaflets of the bilayer. Polarized epithelial cells that often constitute the cellular interface with the environment, have tight junctions, which function to fence off the apical from the basolateral membrane. By virtue of their geometry within the membrane, tight junctions also act to isolate the outer leaflet of the apical membrane, but not the inner, from basolateral

Address correspondence to Warren G. Hill, Laboratory of Epithelial Cell Biology, Renal-Electrolyte Division, University of Pittsburgh School of Medicine, A1222 Scaife Hall, 3550 Terrace Street, Pittsburgh, PA 15261. Fax: (412) 624-5009; E-mail: whill@pitt.edu

membrane lipids (van Meer and Simons, 1986). In this way, a unique outer leaflet lipid composition may be maintained because the tight junction represents a barrier to lateral diffusion. Simons and co-workers have shown that the outer leaflet of epithelial cells are enriched in glycosphingolipids and the inner leaflet in phosphatidylethanolamine and phosphatidylserine (Simons and van Meer, 1988).

To understand the functional consequences of lipid asymmetry and the role it might play in creating a barrier to water permeation, we have previously modeled the inner and outer leaflet of the MDCK Type 1 apical membrane. This membrane has been shown to have extremely low permeabilities for water and solutes (Lavelle et al., 1997), and its lipid composition has been thoroughly characterized (Hansson et al., 1986; van Meer and Simons, 1986). By making liposomes that had the same composition as either the inner or outer leaflet, we were able to test their permeabilities individually and extrapolate a predicted permeability for the MDCK apical membrane (Hill and Zeidel, 2000). Although this approach yielded a value close to that obtained from experimental measurements of the permeability of this membrane, it was based on the theoretical assumption that each leaflet of the bilayer would resist solute permeation independently. We have now tested this assumption directly by creating asymmetric planar bilayers that mimic the MDCK apical membrane and by using a novel technique for measuring water permeability in close proximity to the membrane (Pohl et al., 1997). The results confirm that each leaflet independently resists water permeation, and that the resistance is additive, which is in line with previous predictions (Negrete et al., 1996; Hill et al., 1999; Hill and Zeidel, 2000). We also confirm that the osmotic water permeability coefficient (P_f) for reconstituted MDCK apical membrane derived using leaflet-specific liposomes is comparable to that obtained using asymmetric planar membranes.

MATERIALS AND METHODS

Lipids

The following lipids from Avanti Polar Lipids Inc. were used to construct planar lipid membranes that would reconstitute the MDCK apical membrane: bovine heart phosphatidylethanolamine (Cat. No. 830025), brain phosphatidylserine (Cat. No. 830032), bovine liver phosphatidylinositol (Cat. No. 830042), bovine heart phosphatidylcholine (PC,* Cat. No. 830052), cholesterol (Cat. No. 700000), egg sphingomyelin (Cat. No. 860061), and brain cerebroside (Cat. No. 131303). The lipid composition of the inner and outer leaflets are shown in Table I. Justification for these compositions may be found in Hill and Zeidel (2000).

*Abbreviations used in this paper: CS, cholesterol sulfate; DPPC, dipalmitoylphosphatidylcholine; DPhPC, diphytanylphosphatidylcholine; E_a , activation energy; PC, phosphatidylcholine.

TABLE I
Lipid Composition of Leaflets

Lipids	Exofacial leaflet composition		Cytoplasmic leaflet composition	
	Percent by weight	Mole percent	Percent by weight	Mole percent
PE			48.3	40.1
PS			25.5	20.1
PI			3.6	2.5
Cholesterol	37.3	52.3	22.6	37.3
PC	12.0	8.6		
SM	23.8	18.4		
GSL	26.8	20.7		

Membrane Formation

Planar bilayer membranes were built by the monolayer apposition technique across a 150–250- μm hole in a septum (thickness 25 μm) separating two compartments of a Teflon chamber (Montal and Mueller, 1972). First, equal volumes of hexane (Fluka), methanol (Fluka), and ether (Merck) were used to dissolve the lipid. The solution was spread on the top of the aqueous phase on cis and trans sides of the septum to form lipid monolayers. After evaporating the solvent, the buffer solution levels in both compartments were raised above the aperture using syringes. The septum was pretreated with 2% solution of hexadecane in hexane. Spontaneously, the two monolayers combined to a bilayer within the aperture. Membrane capacitance was continuously monitored applying a 1-kHz sine wave to the membrane. The buffer solutions contained 100 mM sodium chloride (Merck) and 10 mM HEPES (Fluka), pH 7.4. They were agitated by magnetic stirrer bars.

An osmotic gradient was created by addition of urea (Merck) to one side of the membrane only. Because the urea permeability of these membranes was three orders of magnitude smaller than the water permeability (1.6×10^{-6} vs. 4.4×10^{-3} cm/s for cytoplasmic and 3.10^{-8} vs. 2.4×10^{-4} cm/s for exofacial [Hill and Zeidel, 2000]), urea was treated as a nonpermeating solute that was completely reflected by the membrane. The transmembrane urea flux was so small that a diminution of the effective osmotic gradient between bulk solutions (1.5 ml each) did not occur.

Water Flux Measurements

Transmembrane water flux leads to solute concentration changes in the immediate vicinity of the membrane. Water passing through the membrane dilutes the solution it enters and concentrates the solution it leaves (Fettiplace and Haydon, 1980). The near-membrane concentration distribution of any solute can be used to calculate the velocity of the transmembrane water flow, v_t (Pohl et al., 1997). In the present work, v_t was obtained by fitting the sodium concentration profiles to the equation:

$$C(x) = C_s e^{(-v_t x/D) + (ax^3/3D)},$$

where x is the distance from the membrane. D , a , and C_s denote the diffusion coefficient, the stirring parameter, and the solute concentrations at the interface, respectively. Subsequently, v_t allows us to determine the membrane water permeability, P_f :

$$P_f = \frac{v_t}{\chi C_{\text{osm}} V_W},$$

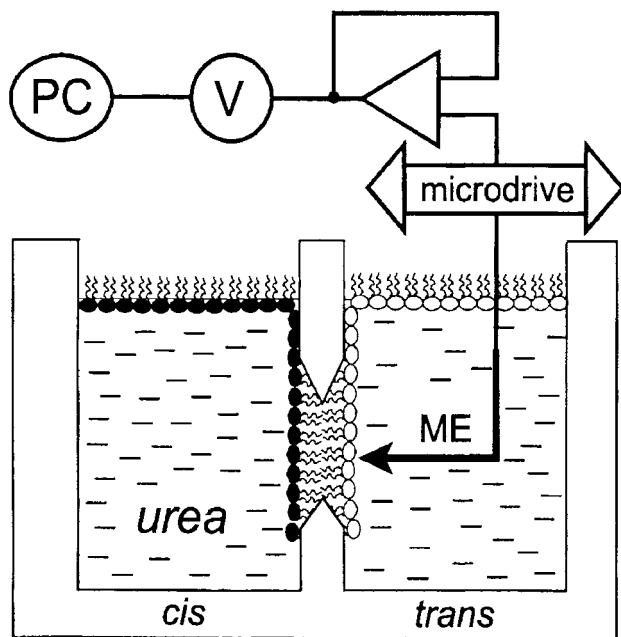


FIGURE 1. Schematic diagram of apparatus used to measure osmotically induced water transport. The sodium concentration in the vicinity of planar lipid membranes was monitored using the microelectrode technique. The membranes were formed by the apposition of two differently composed monolayers within the aperture (diam 150–250 μm) in a polytetrafluoroethylene septum. The microelectrode (ME) was driven to the membrane with the help of a microdrive. The signal was amplified, digitized, and transferred to a personal computer.

where χ , C_{osm} , and V_w are the osmotic coefficient, the near-membrane concentration of the solute used to establish the transmembrane gradient, and the partial molar volume of water, respectively (Pohl et al., 1997).

The sodium concentration distribution in the immediate membrane vicinity was measured using a scanning ion-sensitive microelectrode (Fig. 1). The latter was moved perpendicular to the surface of the membrane by a hydraulic microdrive manipulator (Narishige). The touching of the membrane was indicated by a steep potential change (Antonenko and Bulychev, 1991). From the known velocity of microelectrode motion ($1 \mu\text{m s}^{-1}$), the position of the microsensor relative to the membrane was determined at any instant of the experiment. The accuracy of the distance measurements was estimated to be $\pm 5 \mu\text{m}$. Electrodes with a 90% rise time below 0.6 s were selected. Artifacts due to a very slow electrode motion were therefore unlikely. Nevertheless, possible effects of time resolution or distortion of the stagnant near-membrane water layer were tested by making measurements while moving the microelectrode toward and away from the bilayer. Since no hysteresis was found, it can be assumed that an electrode of appropriate time resolution was driven at a rate that is slow relative to the rate at which any electrode-induced disturbance of the unstirred layer reaches a “stationary” state.

To make the electrode, an aluminosilicate glass capillary tube (Science Products GmbH) was pulled in two stages and silanized by bis-(dimethylamino)-dimethylsilane (Fluka). After bending the tip (outside diam $2 \mu\text{m}$) perpendicular to the rest of the barrel, ion sensitivity was achieved by filling the tip with an ionophore cocktail (sodium ionophore II – cocktail A; Fluka) according to the procedure described by Amman (1986).

Voltage sampling between microelectrode and reference electrode, both of which were placed at the trans side of the bilayer membrane, was performed by a digital multimeter connected to an impedance converter (model AD 549; Analogue Devices). Data was transferred to a personal computer via an RS232 interface.

RESULTS

Planar bilayers, both symmetrical and asymmetrical, formed spontaneously across a small diameter aperture ($\sim 200 \mu\text{m}$) in an apparatus shown schematically in Fig. 1. Water flux across membranes created in this way was

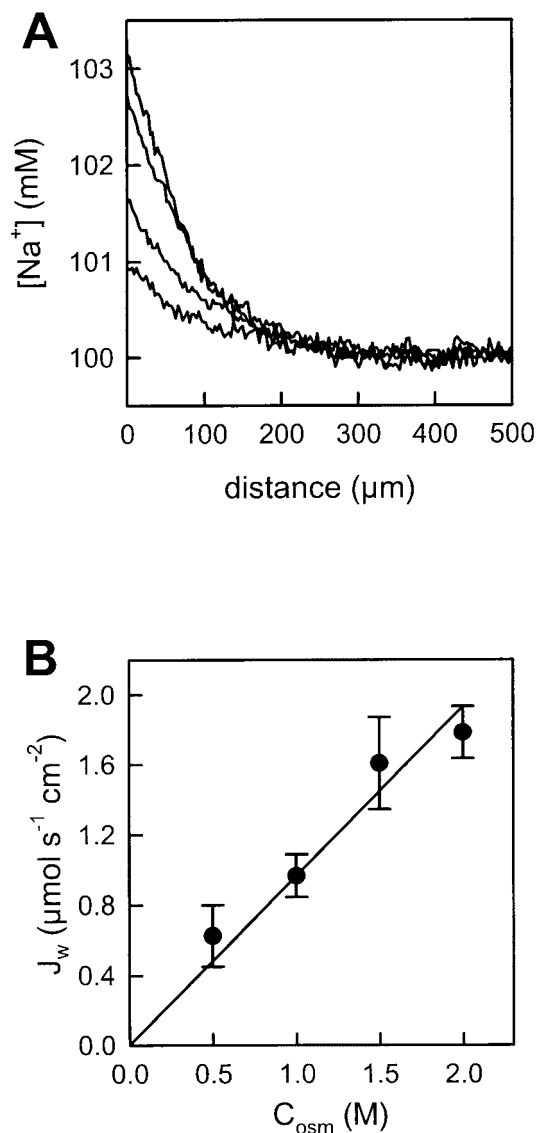


FIGURE 2. Effect of increasing the osmotic gradient on Na^+ concentration profiles in the near vicinity of the membrane. (A) An increase of the urea concentration (0.5, 1.0, 1.5, and 2.0 M) at the cis side of the bilayer lipid membrane was accompanied by an increasing sodium concentration shift within the trans unstirred layer. The membranes were formed from cytoplasmic lipids. The bulk solution contained 100 mM NaCl, 10 mM HEPES, pH 7.4, and the temperature was 28°C . (B) The water flux density (J_w) was proportional to the transmembrane urea gradient.

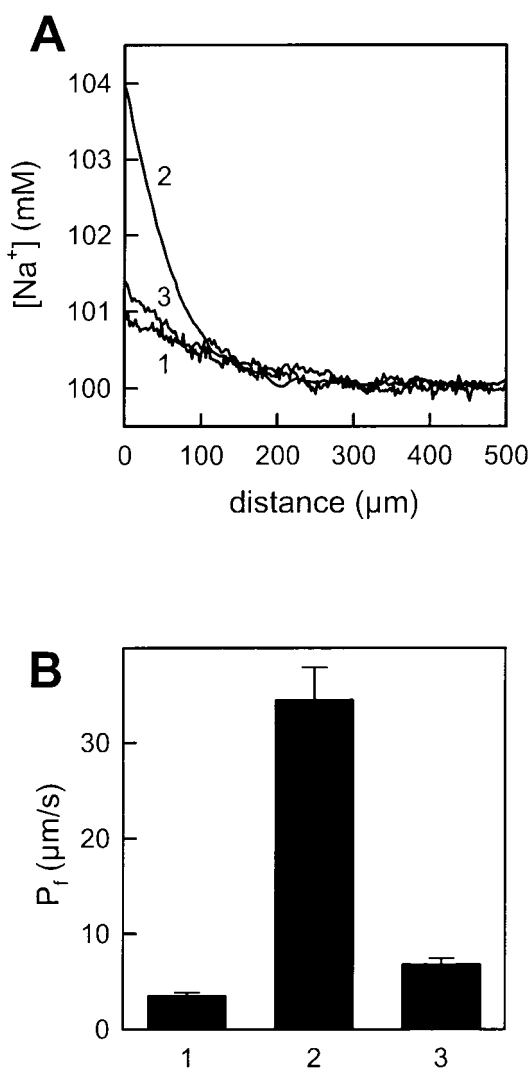


FIGURE 3. Water permeability across symmetric and asymmetric planar lipid membranes. (A) Representative Na^+ concentration profiles at the trans side of BLM induced by the addition of 1 M urea to the cis side. The profiles 1 and 2 correspond to the membranes formed from exofacial and cytoplasmic lipids, respectively, and profile 3 refers to an asymmetrically formed membrane (exofacial lipids [trans monolayer] and cytoplasmic lipids [cis monolayer]). The bulk solution contained 100 mM NaCl, 10 mM HEPES, pH 7.4 and the temperature was 36°C. (B) Water permeability for the different membranes. Error bars represent standard deviations of at least 15 experimental profiles.

induced by urea addition to the cis side of the membrane. During the experiment, membrane capacitance did not change and was equal to $0.82 \pm 0.07 \mu F/cm^2$ for both symmetrical and asymmetrical bilayers.

Water flux across the membrane in response to the osmotic gradient and retention of sodium ions in the trans compartment resulted in an increasing sodium concentration in the immediate membrane vicinity. Representative sodium concentration distributions measured adjacent to a membrane constructed from cytoplasmic lip-

ids are shown in Fig. 2 A. The higher the osmotic gradient imposed, the higher the degree of near-membrane polarization. The transmembrane water flux densities (J_w) were proportional to the effective osmotic gradient (Fig. 2 B). To calculate the latter, the urea gradient was corrected for dilution. Because the diffusion coefficients of urea and sodium are very close, it was assumed that the ratios of their near-membrane and bulk concentrations are identical (Pohl et al., 1998).

Similar measurements in the immediate vicinity of membranes formed from exofacial lipids and for asymmetrical bilayers built from an exofacial and a cytoplasmic leaflet revealed a very small polarization of sodium ions making measurements difficult. This was due to the very low water permeation rate across these "tight" membranes. Facilitating water permeation by increasing the temperature to 36°C resulted in well pronounced and reproducible concentration profiles (Fig. 3 A, curve 1). With a P_f of only $3.4 \pm 0.4 \times 10^{-4} cm/s$, the membranes composed of exofacial lipids revealed the lowest permeability coefficient of the three membranes tested (Fig. 3 B for combined data). In contrast, the water permeability of cytoplasmic bilayers was 10-fold higher at $34.4 \pm 3.5 \times 10^{-4} cm/s$ (Fig. 3 A, curve 2). As predicted, P_f of asymmetrical membranes was not simply the arithmetical mean of the leaflet permeabilities and, indeed, was very close to the concentration curve shown for a symmetric exofacial bilayer (Fig. 3 A, curve 3). Calculation of P_f from the experimental profile revealed a value of $6.7 \pm 0.7 \times 10^{-4} cm/s$ that was close to the permeability of exofacial membranes (Fig. 3 B).

To validate the permeability measurements under different experimental geometries, sodium ion dilution adjacent to the cis membrane-water interface was measured, and the direction of the water flux across the bilayer was changed (by altering the relative position of the cytoplasmic and exofacial monolayers). Identical water permeabilities were obtained under all experimental conditions (data not shown).

The polarization of sodium ions was studied at different temperatures (Fig. 4 A). These experiments permitted calculation of the activation energy (E_a) of transmembrane water transport. The activation energy derived from the slope of the plot in Arrhenius coordinates for cytoplasmic lipids was equal to $14.7 \pm 1.5 kcal/mol$ (Fig. 4 B). Similar experiments with symmetrical exofacial membranes revealed an E_a of $22.1 \pm 3.0 kcal/mol$. Hence, membranes with tighter packing and lower fluidity due to the presence of significant quantities of cholesterol and sphingolipid, have a significantly higher E_a for water permeation. Estimates of water permeability at 25°C for these membranes yield values of $1.36 \times 10^{-3} cm/s$ and $1.0 \times 10^{-4} cm/s$ for cytoplasmic and exofacial bilayers, respectively. These compare favorably with previously measured perme-

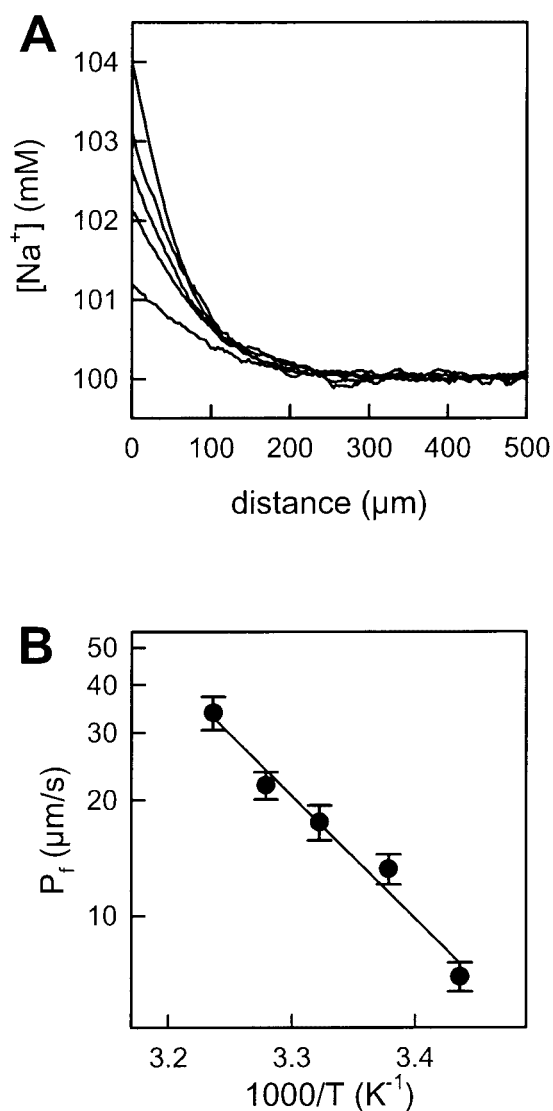


FIGURE 4. Effect of temperature on water permeation. (A) Temperature augmentation (18, 23, 27, 32, and 36°C) promotes the transmembrane water flux. As a result, the sodium concentration polarization in the unstirred layer increased. The membranes were formed from cytoplasmic lipids. The bulk solution contained 100 mM NaCl, 10 mM HEPES, pH 7.4, and additionally 1 M urea at the cis side. (B) Arrhenius plot of water permeability through the BLM. The calculated activation energy was 14.7 ± 1.5 kcal/mol.

abilities in liposomes of 4.4×10^{-3} and 2.4×10^{-4} cm/s, respectively (Hill and Zeidel, 2000).

DISCUSSION

Much of our current understanding of membrane permeation processes has been achieved by studying the permeant behavior of water across simple model lipids like dipalmitoylphosphatidylcholine (DPPC). An understanding of permeant behavior in cellular membranes is, however, a much more difficult challenge. Cell membranes are extremely complex in both their

composition and their structure. In addition to lipids that exhibit variations in head groups, acyl chain lengths, cholesterol concentrations, and degrees of saturation, membranes also exhibit bilayer asymmetry, phase discontinuities, membrane-embedded proteins, and may have their permeation properties affected by extracellular matrix and/or mucus. In these experiments, our aim was to use a novel technique for measuring water permeability across planar bilayers (Pohl et al., 1997), to examine the influence of one of these parameters (bilayer asymmetry) on water permeation across a simplified cell membrane.

Many, if not all cells, are now thought to exhibit differences in the lipid composition of individual leaflets in their plasma membranes (Simons and van Meer, 1988; Roelofsen and Op den Kamp, 1994). Epithelial cells, which are often the interface between the host and the environment, show striking asymmetries in their apical membranes, with high concentrations of glycosphingolipids and sphingomyelin in the outer leaflet. In tissues such as the bladder, the thick ascending limb of Henle, and the kidney collecting duct, the apical membrane must maintain large chemical and osmotic gradients and therefore be effectively impermeable to water. Bilayer lipid asymmetry as generated in the trans-Golgi network and as maintained by tight junctions and the activity of ATP-using phospholipid flippases, represents an elegant way for cells to control the permeability of these critical barrier interfaces (Simons and van Meer, 1988).

Previous studies that have attempted to examine bilayer asymmetry have had limitations. Cholesterol sulfate (CS), which has the advantage of very slow translocation rates from one side of the bilayer to the other, was used to dope one or both sides of planar diphytanlylphosphatidylcholine (DPhPC) membranes. Adding CS to both sides of a DPhPC bilayer reduced diffusive water permeability from 14.9×10^{-4} to 5.4×10^{-4} cm/s. Adding it to one side of the bilayer to induce lipid asymmetry reduced membrane permeability to 8.9×10^{-4} cm/s (Negrete et al., 1996). The authors concluded that the data appeared to support a model of independent resistances being offered by each leaflet. This relation was summarized and expressed as:

$$\frac{1}{P_{AB}} = \frac{1}{P_A} + \frac{1}{P_B}, \quad (1)$$

where P_{AB} is the permeability of a bilayer composed of leaflets A and B, P_A is the permeability of leaflet A, and P_B is the permeability of leaflet B. Unfortunately, the differences between DPhPC bilayers and DPhPC-CS bilayers were modest, and so alternative interpretations were possible. Indeed, the data are equally well explained by an arithmetic mean, which would suggest that the overall permeability of the bilayer is an average

of the permeabilities offered by each leaflet. Bilayer asymmetry also has been artificially induced in DPPC liposomes by addition of the trivalent rare earth metal praseodymium (Negrete et al., 1996; Hill et al., 1999). This reagent was shown to bind to and rigidify the outer leaflet of the liposomes and reduce the overall membrane permeability to water, urea, glycerol, NH_3 , and protons, thus, suggesting that leaflets were contributing independent resistances to permeation. Although functionally inducing a reduction in permeability, it is uncertain how closely this interaction reflects a physiologically relevant phenomenon. Further indirect evidence for Eq. 1 was obtained from studies in which symmetrical liposomes designed to recapitulate the lipid composition of the inner and outer leaflet of MDCK apical membrane were tested for their permeabilities to water and solutes (Hill and Zeidel, 2000). At 25°C, the water permeability of outer leaflet liposomes was 18-fold lower than for inner leaflet liposomes and by using Eq. 1 to extrapolate a predicted asymmetric membrane permeability, a value of 4.6×10^{-4} cm/s was arrived at. This correlated well with measured permeabilities for this membrane that ranged from 1.8 to 10×10^{-4} cm/s (Farinas and Verkman, 1996; Rivers et al., 1996; Timbs and Spring, 1996; Lavelle et al., 1997).

We have now used lipid mixtures that reflect the composition of the MDCK apical membrane inner and outer leaflets and created symmetric and asymmetric planar bilayers from them. By the use of a Na^+ -sensitive microelectrode, which could be positioned within the unstirred layer next to the membrane surface (Fig. 1), it was possible to measure an osmotically induced water flux which was proportional to the size of the osmotic gradient imposed (Fig. 2). This allowed us to test the validity of Eq. 1 as a description for water permeation behavior directly. Measurements of water permeability across symmetric and asymmetric bilayers of MDCK lipids demonstrated a 10-fold difference between inner and outer leaflet membranes at 36°C (Fig. 3 B). An asymmetric membrane composed of an inner and an outer leaflet shows a Na^+ polarization profile far closer to that of outer leaflet lipids than inner leaflet lipids, and this is reflected in a P_f that is only twofold higher (6.7×10^{-4} cm/s compared with 3.4×10^{-4} cm/s). These data indicate that most of the resistance offered by the MDCK apical membrane to water permeation is contributed by the outer leaflet that is enriched in cholesterol and sphingolipids. Application of Eq. 1 to the P_f values calculated from curves 1 and 2 (Fig. 3 B) results in an estimated permeability for the MDCK membrane of 6.2×10^{-4} cm/s, which is extremely close to the measured value of $6.7 \pm 0.7 \times 10^{-4}$ cm/s. We conclude that this data validates the use of Eq. 1 for describing membrane permeation behavior, and that individual leaflets of a bilayer do indeed offer independent and additive

resistances to water permeation. In addition, we believe the results confirm the conclusions reached in earlier studies (Negrete et al., 1996; Hill et al., 1999; Hill and Zeidel, 2000). It is also notable that the values for permeability measured in these bilayers corresponded closely to those obtained in earlier stopped-flow measurements of permeabilities of liposomes of the same compositions (Hill and Zeidel, 2000), thus, validating both approaches for measurement of permeabilities. Keeping in mind that osmotic shock experiments performed with liposomes may be complicated by geometrical changes that are not properly understood, and consequently, volume changes have to be studied by essentially empirical optical methods (Fettiplace and Haydon, 1980), it has to be acknowledged that the coincidence with steady-state microelectrode based flux measurements on planar membranes is reasonable. The latter technique has been approved experimentally by solvent drag experiments. It returns the same flux density for ions that are dragged by water across gramicidin channels as simultaneous current measurements (Pohl and Saparov, 2000).

The E_a for water flux across cytoplasmic lipids is similar to that seen for membranes formed from *Escherichia coli* lipids, as derived from microelectrode measurements on planar membranes (Pohl et al., 2001), or from stopped-flow experiments performed on liposomes (Zeidel et al., 1992). Epithelial plasma membrane vesicles prepared from cells that lack water channels also have been shown to have comparable values (Yano et al., 1996; Alves et al., 1999). Exofacial lipids exhibited a much higher E_a of 22.1 kcal/mol, which is likely to be a reflection of the tighter lipid packing. Increasing amounts of cholesterol were reported to increase the activation energy for PC membranes from ~ 10 to ~ 21 kcal/mol (for a review see Fettiplace and Haydon, 1980). In the exofacial lipid bilayers tested here, it may be the hydrogen-bonding interactions that occur between cholesterol and the sphingolipids which increases E_a over that observed for cytoplasmic lipids.

These results demonstrate that outer leaflets act as the major barrier to permeation across barrier apical membranes. In cells specialized to serve as barriers to water flux, such as the collecting duct in the absence of antidiuretic hormone, the thick ascending limb of Henle, the bladder, and the stomach, the process by which the cell achieves barrier function appears to be the segregation of specific lipids into the outer leaflet of the apical membrane. From studies examining the effects of lipid composition on permeabilities (Lande et al., 1995; Hill and Zeidel, 2000), these epithelia must segregate phosphatidylcholine with nearly completely saturated fatty acids, plus sphingomyelin, cholesterol and glycosphingolipids, within the outer leaflet. Cells achieve this segregation by placing these lipids in what will be the outer leaflet dur-

ing membrane formation in the Golgi, and through the activity of phospholipid flippases in the Golgi and in the plasma membrane itself. Although cholesterol can rapidly exchange between bilayer leaflets, its tight interaction with sphingomyelin maintains a large gradient for cholesterol between outer and inner leaflets of the bilayer. As another consequence of the role of the outer leaflet in barrier function, the inner leaflet of apical membranes of barrier epithelia, does not need to exhibit low permeabilities. Accordingly, this leaflet may be as fluid as the inner leaflets of other cells, permitting it to participate in cell signaling, and perhaps the regulation of membrane proteins.

We thank Dr. John Mathai for useful discussions.

This work was supported by a Research Fellowship from the National Kidney Foundation (to W.G. Hill) and by the National Institutes of Health Grant DK43955. Financial support of the Deutsche Forschungsgemeinschaft (Po 533/2-3 and Po 533/7-1) is gratefully acknowledged.

Submitted: 14 June 2001

Revised: 14 August 2001

Accepted: 14 August 2001

REFERENCES

- Alves, P., G. Soveral, R.I. Macey, and T.F. Moura. 1999. Kinetics of water transport in eel intestinal vesicles. *J. Membr. Biol.* 171:177–182.
- Amman, D. 1986. Ion-Selective Microelectrodes. Principles, Design and Application. Springer, Berlin. 346 pp.
- Antonenko, Y.N., and A.A. Bulychev. 1991. Measurements of local pH changes near bilayer lipid membrane by means of a pH microelectrode and a protonophore-dependent membrane potential. Comparison of the methods. *Biochim. Biophys. Acta.* 1070:279–282.
- Farinas, J., and A.S. Verkman. 1996. Cell volume and plasma membrane osmotic water permeability in epithelial cell layers measured by interferometry. *Biophys. J.* 71:3511–3522.
- Fettiplace, R., and D.A. Haydon. 1980. Water permeability of lipid membranes. *Physiol. Rev.* 60:510–550.
- Finkelstein, A. 1987. Water Movement Through Lipid Bilayers, Pores and Plasma Membranes. Theory and Reality. Wiley-Interscience, New York. 228 pp.
- Hansson, G.C., K. Simons, and G. van Meer. 1986. Two strains of the Madin-Darby canine kidney (MDCK) cell line have distinct glycosphingolipid compositions. *EMBO J.* 5:483–489.
- Hill, W.G., and M.L. Zeidel. 2000. Reconstituting the barrier properties of a water-tight epithelial membrane by design of leaflet-specific liposomes. *J. Biol. Chem.* 275:30176–30185.
- Hill, W.G., R.L. Rivers, and M.L. Zeidel. 1999. Role of leaflet asymmetry in the permeability of model biological membranes to protons, solutes, and gases. *J. Gen. Physiol.* 114:405–414.
- Lande, M.B., J.M. Donovan, and M.L. Zeidel. 1995. The relationship between membrane fluidity and permeabilities to water, solutes, ammonia, and protons. *J. Gen. Physiol.* 106:67–84.
- Lavelle, J.P., H.O. Negrete, P.A. Poland, C.L. Kinlough, S.D. Meyers, R.P. Hughey, and M.L. Zeidel. 1997. Low permeabilities of MDCK cell monolayers: a model barrier epithelium. *Am. J. Physiol.* 273:F67–F75.
- Montal, M., and P. Mueller. 1972. Formation of bimolecular membranes from lipid monolayers and a study of their electrical properties. *Proc. Natl. Acad. Sci. USA.* 69:3561–3566.
- Negrete, H.O., R.L. Rivers, A.H. Goughs, M. Colombini, and M.L. Zeidel. 1996. Individual leaflets of a membrane bilayer can independently regulate permeability. *J. Biol. Chem.* 271:11627–11630.
- Pohl, P., and S.M. Saparov. 2000. Solvent drag across gramicidin channels demonstrated by microelectrodes. *Biophys. J.* 78:2426–2434.
- Pohl, P., S.M. Saparov, and Y.N. Antonenko. 1997. The effect of a transmembrane osmotic flux on the ion concentration distribution in the immediate membrane vicinity measured by microelectrodes. *Biophys. J.* 72:1711–1718.
- Pohl, P., S.M. Saparov, and Y.N. Antonenko. 1998. The size of the unstirred layer as a function of the solute diffusion coefficient. *Biophys. J.* 75:1403–1409.
- Pohl, P., S.M. Saparov, M.J. Borgnia, and P. Agre. 2001. High selectivity of water channel activity measured by voltage clamp: analysis of planar lipid bilayers reconstituted with purified AqpZ. *Proc. Natl. Acad. Sci. USA.* 98:9624–9629.
- Rivers, R.L., J.A. McAteer, J.L. Clendenon, B.A. Connors, and J.C. Williams. 1996. Apical membrane permeability of MDCK cells. *Am. J. Physiol.* 271:C226–C234.
- Roelofsen, B., and J.A. Op den Kamp. 1994. Plasma membrane phospholipid asymmetry and its maintenance: the human erythrocyte as model. In *Cell Lipids*. D. Hoekstra, editor. Academic Press Inc., San Diego. 7–46.
- Simons, K., and G. van Meer. 1988. Lipid sorting in epithelial cells. *Biochemistry.* 27:6197–6202.
- Smaby, J.M., H.L. Brockman, and R.E. Brown. 1994. Cholesterol's interfacial interactions with sphingomyelins and phosphatidylcholines: hydrocarbon chain structure determines the magnitude of condensation. *Biochemistry.* 33:9135–9142.
- Smaby, J.M., M. Momsen, V.S. Kulkarni, and R.E. Brown. 1996. Cholesterol-induced interfacial area condensations of galactosylceramides and sphingomyelins with identical acyl chains. *Biochemistry.* 35:5696–5704.
- Timbs, M.M., and K.R. Spring. 1996. Hydraulic properties of MDCK cell epithelium. *J. Membr. Biol.* 153:1–11.
- van Meer, G., and K. Simons. 1986. The function of tight junctions in maintaining differences in lipid composition between the apical and basolateral cell surface domains of MDCK cells. *EMBO J.* 5:1455–1464.
- Yano, M., R.A. Marinelli, S.K. Roberts, V. Balan, L. Pham, J.E. Tarara, P.C. de Groen, and N.F. LaRusso. 1996. Rat hepatocytes transport water mainly via a non-channel-mediated pathway. *J. Biol. Chem.* 271:6702–6707.
- Zeidel, M.L., S.V. Ambudkar, B.L. Smith, and P. Agre. 1992. Reconstitution of functional water channels in liposomes containing purified red cell CHIP28 protein. *Biochemistry.* 31:7436–7440.